

# The Influence of Riblets on the Development of a $\Lambda$ Structure and Its Transformation into a Turbulent Spot

Yu. A. Litvinenko<sup>a</sup>, V. G. Chernoray<sup>a</sup>, V. V. Kozlov<sup>a</sup>, L. Loef Dahl<sup>b</sup>,  
G. R. Grek<sup>a</sup>, and H. H. Chun<sup>c</sup>

Presented by Academician A.K. Rebrov July 13, 2005

Received August 31, 2005

PACS numbers: 47.27.Cn, 47.32.C–

DOI: 10.1134/S1028335806030128

Riblets are passive elements mounted on a smooth wall surface in a turbulent boundary layer, which can reduce friction drag up to 10%. These elements have the form of streamwise grooves with triangular or hemispherical cross section whose dimensions are comparable with those of a viscous sublayer. The systematic investigations of riblets as a means of reducing turbulent friction began in the late 1970s at the NASA Research Center in Langley [1–4]. These investigations showed that the friction drag decreases when the dimensionless parameter of riblets  $s^+ = \frac{su^*}{\nu}$  is approx-

imately equal to 15. However, the drag increases at  $s^+ = 30$ . For the maximum drag reduction, the riblets must be oriented in the direction of the local velocity of the viscous sublayer. The net drag reduction is almost linearly proportional to the coverage of the entire streamlined surface by the riblets.

The near-wall turbulent structure of flows on riblets was extensively studied using physical [3, 5, 6] and numerical experiments (DNS) [7, 8]. According to one of the hypotheses put forward in order to explain the drag reduction in the turbulent boundary layer on riblets, they modify coherent structures in the viscous sublayer. It was found that riblets operate as an obstacle for the transversal (spanwise) oscillations of streamwise vortices, which results in drag reduction [9]. In other words, riblets reduce the friction drag in the turbulent boundary layer by changing the sequence of the near-wall vortex dynamics by means of a passive spanwise

forcing. Numerical experiments showed [10] that there develops a process reducing the streamwise vorticity  $\omega'_x$  on riblets.

Thus, the hypothesis according to which the friction drag is reduced by riblets in the turbulent boundary layer as a result of their action on the coherent structures in the viscous sublayer is confirmed in both numerical and physical experiments. In [11], the authors obtained a 10% reduction of the turbulent friction by suppressing the spanwise oscillations between riblet grooves. A considerable reduction of the  $\omega$  pulsations of the velocity by riblets was also observed in [12].

Coherent vortex structures also exist in transition boundary layers. The first attempts to control their development using riblets to provide for a delay in the transition to turbulence were carried out in [13–15]. In a physical experiment [13], it was shown that riblets destabilize the flow in a laminar boundary layer at the linear stage of development of Tollmien–Schlichting waves and stabilize it at the nonlinear stage, when streamwise  $\Lambda$ -shaped vortex structures appear [13]. Naturally, the characteristic dimensions of riblets for a transition boundary layer differ from those used in a turbulent boundary layer. A certain measure is provided by the scale of thicknesses of a laminar viscous sublayer in the turbulent boundary layer and a laminar boundary layer. The riblet heights in the former case usually amount to 30–50% of the thickness of the viscous sublayer (which is typically about 20–30  $\mu\text{m}$ ). In the case of a laminar boundary layer, the proportion is the same (30–50%), but with respect to a thickness that is greater by one and a half orders of magnitude. In preliminary experiments [13], the optimal configuration of riblets and their spatial dimensions (on the order of 1000  $\mu\text{m}$ ) were chosen. The experimental investigations showed the stabilizing effect of these riblets on the transition to turbulence in flows with coherent struc-

<sup>a</sup> *Institute of Theoretical and Applied Mechanics, Siberian Division, Russian Academy of Sciences, ul. Institutskaya 4/1, Novosibirsk, 630090 Russia*

<sup>b</sup> *Chalmers University of Technology, Göteborg 41296, Sweden*

<sup>c</sup> *Pusan National University, Pusan, Korea*

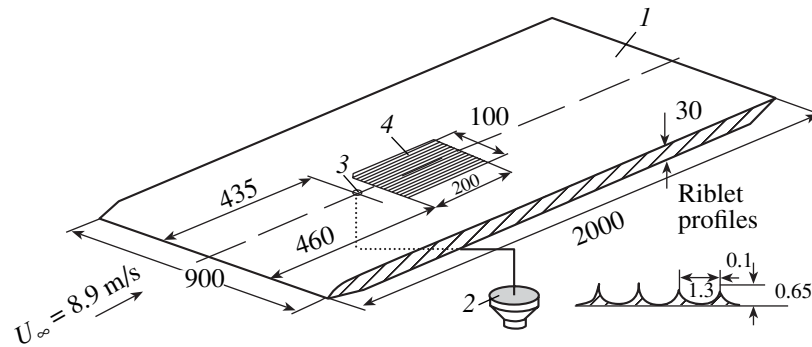


Fig. 1. Experimental set-up (see the text for explanations).

tures of the type of  $\Lambda$ - and  $\Omega$ -shaped vortices, streaky structures, and stationary streamwise vortices of the Görtler flow type. It was noted that this effect was related, in particular, to the suppression of the spanwise velocity gradient, that is, to an increase in the flow stability with respect to the development of secondary high-frequency perturbations and, consequently, to a delay in the turbulization of flows. In the case of riblets affecting the development of a single  $\Lambda$  structure or a group of  $\Lambda$  structures in the K transition regime, it was shown that riblets delay their transformation into turbulent spots, especially in the latter situation [13]. Thus, it was found that riblets render favorable effect on the turbulent transition at the linear stage of the classical transition and in the flows with coherent structures.

This paper presents the results of detailed experimental investigations of the effect of riblets on the development of a  $\Lambda$  vortex structure and its transformation into a turbulent spot. The experiments were performed using modern methods of experimental data acquisition, processing, and representation. For this purpose, we measured the streamwise component of the mean velocity and the velocity fluctuations in space ( $xyz$ ) at various moments of time. This made it possible to obtain the spatiotemporal patterns of the  $\Lambda$  structure development on smooth and ribbed surfaces and represent them as hot-wire visualization of the flow structure evolution in space and time, as well as of contour diagrams of constant velocity fluctuations.

The experiments were performed under controlled conditions in a low-turbulence wind tunnel. A flat plate  $l$  (30 mm thick, 900 mm wide, and 2000 mm long) was mounted and oriented streamwise in the working part of the tunnel (Fig. 1). The  $\Lambda$ -shaped vortex structure was generated using gas blow-in by a dynamic loudspeaker 2 through a 3-mm hole 3 located at the center of the plate at a distance of  $x = 435$  mm from its leading edge. The dynamic loudspeaker was driven by an electric signal having the form of rectangular pulses supplied at a repetition rate of 4 Hz. The pulses provided the generation of spatially localized perturbations. In order to ensure more reliable stabilization of the signal for its averaging over the ensemble, as well as to pro-

vide a controlled secondary disturbance leading to breakdown of the  $\Lambda$  structure and its transformation into a turbulent spot, the rectangular pulses were modulated by a secondary high-frequency perturbation with a small amplitude and a frequency of 240 Hz. In the absence of such modulation, we failed to eliminate the background noise at the final stages of the  $\Lambda$  structure transformation into a turbulent spot. A riblet insert 4, which was mounted at a distance of 25 mm from the point where the disturbances were introduced, represented a rectangular pad with dimensions  $200 \times 100$  mm. The insert was flash-mounted in such a way that the valleys of riblets were leveled with the surface of the plate (i.e., the bottom of the insert was depressed). The riblet height was  $h = 0.65$  mm, the spacing between neighboring peaks was  $s = 1.3$  mm, and the rib top width was 0.1 mm (see the inset in Fig. 1). The dimensionless parameter of the riblets is defined as  $s^+ = \frac{su^*}{\nu}$ , where

$u^* = \left( \nu \left| \frac{\partial u}{\partial y} \right|_{y=0} \right)^{1/2}$  is the velocity of the laminar flow,

$\left| \frac{\partial u}{\partial y} \right|_{y=0} = \frac{0.332 U_\infty}{\delta}$  is the gradient of the mean veloc-

ity at the wall, and  $\delta \sim \left( \frac{\nu X}{U_\infty} \right)^{1/2}$ . In the range of Rey-

nolds numbers under investigation,  $Re_x = (2.82-3.77) \times 10^5$ , the dimensionless parameter  $s^+$  normalized to the internal variables ( $\nu, u^*$ ) was within  $19 \geq s^+ \geq 18$ . This value is rather close to the analogous parameter ( $26 \geq s^+ \geq 21$ ) determined in [13] and approaches the optimal parameter of riblets for the turbulent boundary layer ( $s^+ = 15$ ) reported in [1]. The flow velocity was  $U_\infty = 8.9$  m/s and the turbulence level did not exceed 0.04%. A heat-loss anemometer measured the time-average streamwise velocity component  $U$  and the velocity fluctuations  $u'$ . For all the measurements, the coordinates  $x$  are indicated relative to the position of the perturbation source (3-mm hole located at a distance of 435 mm from the leading edge of the plate).

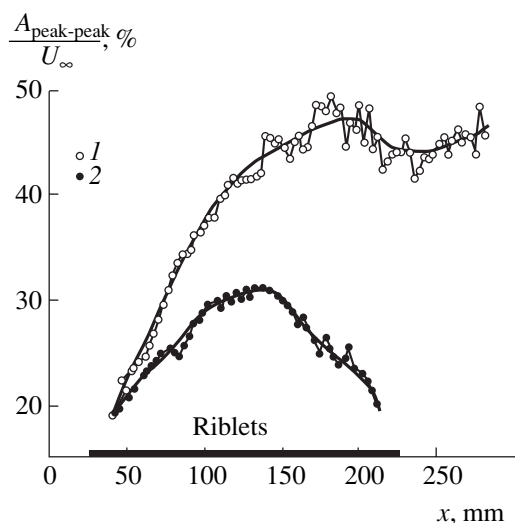


**Fig. 2.** Growth rates of the  $\Lambda$ -structure intensity downstream on the (1) smooth and (2) ribbed surfaces of a flat plate for a free stream velocity of  $U_\infty = 8.9$  m/s.

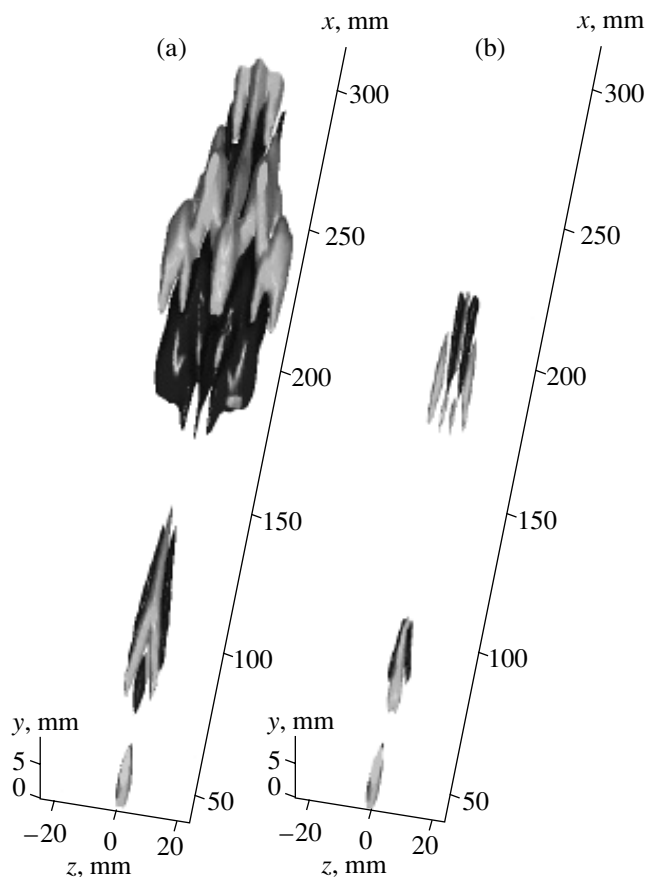


**Fig. 3.** Spatial patterns of the hot-wire visualization of the  $\Lambda$ -structure the development on the (a) smooth and (b) ribbed surfaces of a flat plate at  $x = 40, 75$ , and  $175$  mm; the amplitude levels of the isosurfaces is  $0.025U_\infty$ ;  $U_\infty = 8.9$  m/s (the dark and light halftones correspond to increased and decreased velocities, respectively).

Let us consider the results of our investigation in some detail. The study of the flow structure in the boundary layer on the smooth and ribbed surfaces of the flat plate showed that the flow is laminar and the velocity profile is close to that in the Blasius boundary layer. The pattern of generated perturbations mapped by the isolines of velocity fluctuations at the point of the beginning of measurements ( $x = 40$  mm) on both smooth and ribbed surfaces of the plane plate at  $z = 0$  demonstrates that, in both cases, the flow structure remains virtually unchanged. In other words, at the initial stage of development of perturbations, the riblets did not produce any noticeable effect on the flow structure. On the other hand, the identity of the initial conditions of the experiment was the same. Figure 2 shows the dependences of the intensity of perturbations developed on the smooth and ribbed surfaces on the longitudinal coordinate  $x$ . For the same initial value ( $0.19U_\infty$  at  $x = 40$  mm), the amplitude of perturbations on the smooth surface sharply increases (to  $0.47U_\infty$  at  $x = 200$  mm) and a turbulent breakdown of the structure is observed downstream. On the contrary, in the presence of riblets, the initial growth of the perturbation amplitude is arrested (at  $0.31U_\infty$  at  $x = 140$  mm) and then it begins to fall at the same rate until reaching the initial value at the end of the riblet insert ( $0.19U_\infty$  at  $x = 210$  mm). Thus, the riblets favor a more than twofold decrease in the intensity of initial perturbations, thereby stabilizing the flow (see Fig. 2).

Now let us consider the dynamics of the development of localized perturbations on the smooth and ribbed surfaces, as reflected by the isosurfaces of velocity fluctuations ( $0.025U_\infty$ ) in space ( $xyz$ ). Figure 3 shows the results of measurements at various positions downstream. Using Fig. 3a, it is possible to compare the structure of perturbations at the beginning and at the end of their development on the smooth surface (in the streamwise direction). It is clearly seen that the  $\Lambda$  structure generated in the beginning (at  $x = 40$  and  $75$  mm) transforms downstream into a complex pattern consisting of a number of coherent structures at  $x = 175$  mm. Usually, such a pattern is observed for a turbulent spot averaged over an ensemble. Moreover, the turbulent velocity fluctuations was observed on the signal oscillograms in this region, which makes it possible to ascertain that the  $\Lambda$  structure moving downstream exhibits transformation into a turbulent spot.

A more detailed analysis of the pattern of evolution of the localized perturbations downstream at various coordinates  $x$  on the smooth and ribbed surfaces shows that, at  $x = 40$  mm, the structure of the disturbance in both cases remains unchanged. However, on moving downstream, the  $\Lambda$  structure on the smooth surface transforms into a complex pattern characterized by a large number of regions of defect and excess velocity and by a progressive increase in the streamwise and spanwise perturbation scales. Eventually, the  $\Lambda$  structure gradually transforms into a solitary turbulent spot observed at  $x = 175$  mm. It is also necessary to note a lon-

itudinal stretching of the  $\Lambda$  structure ( $x = 75$  mm) that is typical of the  $\Lambda$  vortex transformation into a so-called hairpin vortex in a downstream shear flow. In contrast to this pattern, the structure of the  $\Lambda$  vortex moving downstream on the riblet surface exhibits rather small variations. The spanwise and streamwise scales change insignificantly, and finally (see Fig. 3b,  $x = 175$  mm), it is seen that the  $\Lambda$  structure is virtually unable to transform into a turbulent spot in this situation.

The maps of isolines of velocity fluctuations obtained during the development of the  $\Lambda$  structure moving downstream on the smooth and ribbed surfaces demonstrate that the structure of perturbations in both cases represent closed regions of decreased and increased velocity, which are located strictly symmetrically about its plane of symmetry. The characteristic features of the development of the  $\Lambda$  structure on the smooth and ribbed surfaces, which are revealed by the patterns of the isosurfaces of velocity fluctuations in space ( $xyz$ ), can also be observed in this situation. In addition, one can note the presence of oblique waves generated both by the  $\Lambda$  structure and by the turbulent spot. On the diagrams, this is reflected by the appearance of regions of defect and excess velocity on each side at the periphery of the basic structures. On the whole, the results of measurements showed that riblets provide an effective means of controlling the development of the  $\Lambda$  structure and its transformation into a turbulent spot.

On a higher level of investigations (with computer-controlled acquisition, processing, and spatiotemporal representation of experimental data), the obtained results confirmed the conclusion made in [13] about the stabilizing effect of riblets on the development of non-stationary vortex objects of the  $\Lambda$  vortex type. We obtained quantitative information about the mechanism of suppression of the process of  $\Lambda$  structure transformation into a turbulent spot on riblets. Thus, the hypothesis concerning the stabilizing effect of riblets on the development of coherent structures in a viscous sublayer in the turbulent boundary layer is once more confirmed in experiments on the controlled development of a coherent structure of the laminar-turbulent transition in the boundary layer on a ribbed surface.

In conclusion, it should be noted that the results of our experiments showed that the  $\Lambda$  structure is transformed into a turbulent spot downstream on a smooth surface of a flat plate. In the case of a ribbed surface, it is found that riblets prevent the transformation of the  $\Lambda$  structure into a turbulent spot and lead to a decay of this perturbation. It is found that the intensity of the  $\Lambda$  structure on riblets initially increases and then decays (at

about 180 mm downstream) to less than half of the level observed in the case of perturbation development on a smooth surface. It is found that the  $\Lambda$  structure is stretched downstream on a smooth surface and transforms into a hairpin vortex. In both cases (i.e., for smooth and ribbed surfaces), the single  $\Lambda$  structure and the turbulent spot generate oblique waves at the periphery.

## ACKNOWLEDGMENTS

This work was supported by the Russian Foundation for Basic Research (grant no. 05-01-00034), the Program of Support for Leading Scientific Schools (NSH-964.2003.1), and by the Advanced Ship Engineering Research Center of the Korea Science and Engineering Foundation.

## REFERENCES

1. M. J. Walsh, in *Viscose Drag Reduction*, Ed. by G. R. Hough (AIAA, Washington, 1980), pp. 168–184.
2. M. J. Walsh, AIAA Pap. 82-0169 (AIAA, Reston, 1982).
3. M. J. Walsh, in *Viscose Drag Reduction in Boundary Layers, Progress in Astronautics and Aeronautics*, Ed. by B. J. Hefner (AIAA, Reston, 1998), p. 123.
4. M. J. Walsh and A. M. Lindeman, AIAA Pap. 84-0347 (AIAA, Reston, 1984).
5. E. Coustols and M. Savill, VKI Lect. Ser. Notes, Report No. 786-8, 1 (1992).
6. E. Coustols, in *Emergent Techniques in Drag Reduction*, Ed. by K. S. Choi, K. K. Prasad, and T. V. Truong (MEP, London, 1996), pp. 3–43.
7. H. Choi, P. Moin, and J. Kim, *J. Fluid Mech.* **255**, 503 (1993).
8. D. Goldstein, R. A. Handler, and L. Sirovich, *J. Fluid Mech.* **302**, 333 (1995).
9. K. S. Choi, in *Transport Phenomena in Turbulent Flows*, Ed. by M. Hirata and N. Kasagi (Hemisphere, New York, 1987), pp. 185–198.
10. C. H. Ph. Crawford, PhD Thesis (Princeton Univ., New Jersey, 1996).
11. D. W. Berhert, M. Bruse, W. Hage, et al., *J. Fluid Mech.* **338**, 59 (1997).
12. Y. Suzuki and N. Kasagi, *AIAA J.* **32**, 1781 (1994).
13. G. R. Grek, V. V. Kozlov, and S. V. Titarenko, *J. Fluid Mech.* **315**, 31 (1996).
14. G. R. Grek, V. V. Kozlov, and S. V. Titarenko, *Rech. Aerosp.*, No. 1, 1 (1996).
15. G. R. Grek, V. V. Kozlov, B. G. B. Klingmann, and S. V. Titarenko, *Phys. Fluids* **7** (10), 2504 (1995).

*Translated by Yu. Vishnyakov*